Earth-based detection of Uranus' aurorae

L. Lamy,[1] R. Prangé,[1] K. C. Hansen,[2] J. T. Clarke,[3] P. Zarka,[1] B. Cecconi,[1] J. Aboudarham,[1]
N. André,[4] G. Branduardi-Raymont,[5] R. Gladstone,[6] M. Barthélémy,[7] N. Achilleos,[8]
P. Guio,[8] M. K. Dougherty,[9] H. Melin,[10] S. W. H. Cowley,[10] T. S. Stallard,[10]
J. D. Nichols,[10] and G. Ballester[11]

[1] This study is based on multi-planet multi-wavelength observations of planetary aurorae throughout the heliosphere, acquired along the propagation path of a series of consecutive interplanetary shocks. The underlying motivation to track the shocks was to increase the probability of detection of auroral emissions at Uranus. Despite several Earth-based attempts in the past few years, at Far-UV (FUV) and Near-IR (NIR) wavelengths, such emissions have never been unambiguously re-observed since their discovery by Voyager 2 in 1986. Here, we present a campaign of FUV observations of Uranus obtained in November 2011 with the Hubble Space Telescope (HST) during active solar wind conditions. We positively identify auroral signatures in several of these HST measurements, together with some obtained in 1998, representing the first images of Uranus' aurorae. We analyze their characteristics and discuss the implications for the asymmetric Uranian magnetosphere and its highly variable interaction with the solar wind flow from near-solstice (1986) to near-equinox (2011) configurations. **Citation:** Lamy, L., et al. (2012), Earth-based detection of Uranus' aurorae, *Geophys. Res. Lett.*, *39*, L07105, doi:10.1029/2012GL051312.

1. Introduction

[2] Among the known planetary magnetospheres, the unique case of Uranus has been scarcely studied, because of its large distance from Earth. Its magnetosphere has been investigated in detail only once, in January 1986 during the Voyager 2 flyby, which revealed a highly tilted (59°) and offset (−0.3 Uranian radii, 1 R_U = 25559 km) magnetic axis

[1]LESIA, Observatoire de Paris, CNRS, UPMC, Université Paris Diderot, Meudon, France.
[2]Department of Atmospheric, Oceanic and Space Sciences, University of Michigan, Ann Arbor, Michigan, USA.
[3]Center for Space Physics, Boston University, Boston, Massachusetts, USA.
[4]Institut de Recherche en Astrophysique, CNRS, Université Paul Sabatier, Toulouse, France.
[5]Mullard Space Science Laboratory, University College London, Dorking, UK.
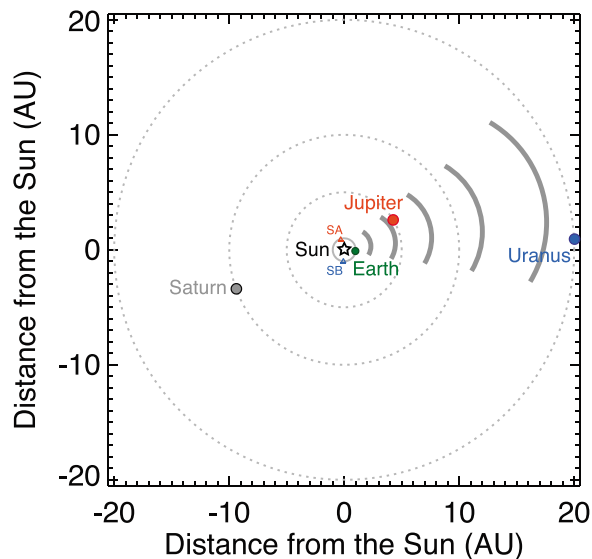[6]Southwest Research Institute, San Antonio, Texas, USA.
[7]Institut de Planétologie et d'Astrophysique de Grenoble, CNRS, Université Joseph Fourier, Grenoble, France.
[8]Department of Physics and Astronomy, University College London, London, UK.
[9]Blackett Laboratory, Imperial College London, London, UK.
[10]Department of Physics and Astronomy, University of Leicester, Leicester, UK.
[11]Lunar and Planetary Laboratory, University of Arizona, Tucson, Arizona, USA.

with respect to the spin axis [*Ness et al.*, 1986; *Connerney et al.*, 1987]. Combined with the large obliquity of the latter (98°, close to the ecliptic plane), this results in an asymmetric magnetosphere very different from the cases of the Earth, Jupiter or Saturn, and only remotely comparable to Neptune. At that time, Uranus lay close to solstice with its northern rotation pole pointing nearly toward the Sun, and its magnetic axis remaining at large angles to the solar wind direction.

[3] Anticipated from IUE observations of variable H Lyman-α emission [*Clarke et al.*, 1986], Uranian aurorae were first unambiguously identified by the Voyager 2 UV spectrometer (UVS) as bright emissions in H Ly-α and H_2 bands around both magnetic poles [*Broadfoot et al.*, 1986]. These data were extensively analyzed by *Herbert and Sandel* [1994] and *Herbert* [2009]. Northern (N) and Southern (S) auroral ovals lie on conjugate field lines at 60° to 65° magnetic latitude (L = 5 to 10 R_U). Because of the peculiar magnetic topology, they are located closer to the spin equator than to the uranographic poles, at planetocentric latitudes ranging from −30° to +50° and from −70° to −30°, the "weak-field" N oval being larger than the "strong-field" S oval. In addition, observed N and S emissions do not form complete ovals, being rather enhanced in the magnetotail direction. This property suggested a prominent role for solar wind convection driving particle acceleration, while the longitudinal elongation of the enhanced sector (up to 180°) suggested the presence of an Earth-like partial ring current. N and S aurorae were found to radiate 3 and 7 $\times$ 10^9 W over the band 87.5–125 nm (including H Ly-α), being more intense around the nightside strong-field S pole. Voyager 2 magnetic and radio measurements were used to determine the planetary rotation period of 17.24 ± 0.01 h [*Desch et al.*, 1986], and define a Uranian longitude system (ULS, in which the north points along the spin axis). In this system, N and S magnetic poles lie at +15.2° and −44.2° latitude. The uncertainty of ULS longitudes today exceeds several rotations, such that the rotational phase of the magnetic poles is lost.

[4] Since Voyager 2, two attempts have been made to re-observe Uranus' Far-UV (FUV) aurorae with the Hubble Space Telescope (HST), once in 1998 with the Space Telescope Imaging Spectrograph (STIS, program 7439, PI: G. Ballester) and again in 2005 with the Advanced Camera for Surveys (ACS, program 10502, PI: J. Clarke), but without reporting any positive detection. In parallel, long-term ground-based observations at near-IR (NIR) wavelengths revealed variations in the thermospheric emission of the H_3^+ molecule, part of which (∼20%) was attributed to auroral precipitations [*Lam et al.*, 1997; *Trafton et al.*, 1999;

Figure 1. Planetary configuration in late 2011. A 50° wide CME propagating radially toward Uranus is shown in dark gray. SA and SB indicate STEREO A and B.

Melin et al., 2011]. As a result, our knowledge of the magnetosphere remains essentially based on the few hours of observations acquired 26 years ago. Moreover, Uranus is now close to equinox, a situation radically different from solstice conditions prevailing in 1986 (a Uranian revolution lasts 84 years), which has never been investigated.

[5] This motivated a new attempt to observe Uranian aurorae with HST, as this telescope remains the most powerful available UV observatory and possesses enough sensitivity to detect the faint emissions recorded by Voyager 2/UVS. The methodology used for scheduling this campaign is presented in section 3, while the results obtained are presented in section 4 and discussed in section 5.

2. Scheduling the Observations Through Solar Wind Tracking

[6] Compressions of planetary magnetospheres by the solar wind flow act as drivers of energetic particle precipitation, which trigger enhanced auroral emissions over a wide range of wavelengths. Activated along high-ram pressure interplanetary shock paths, planetary aurorae thus form a valuable diagnostic to remotely probe solar wind conditions throughout the heliosphere. As an illustration, *Prangé et al.* [2004] a posteriori identified the successive auroral responses of the Earth (in UV), Jupiter (in radio) and Saturn (in UV), coincidently quasi-aligned, along the propagation of a series of solar coronal mass ejections (CME) emitted in November 2000.

[7] Assuming that this overall property similarly applies to Uranus, our methodology was to track high-ram pressure shocks and propagate them to the planet to predict optimal periods for the detection of faint auroral signatures, instead of observing randomly. This approach was successfully used once for Saturn in February 2007 [*Clarke et al.*, 2009]. To predict a period of interest, solar wind data were monitored at Earth and then propagated to the outer solar system using the 1D MHD mSWiM model [*Zieger and Hansen*, 2008]. This code, previously validated with propagations up to 10 AU (Saturn), was here extended up to 19 AU (Uranus) by

including a torus model of heliospheric neutrals beyond Saturn's orbit, which marginally affects final results. To achieve the most accurate propagations while minimizing HST contamination by Earth's geocorona, observations had to be scheduled close to Uranus opposition (on 26 September 2011). Fortunately, Jupiter was quasi-aligned with the Earth and Uranus at the same epoch, providing the opportunity to remotely sense the Jovian auroral response to solar wind at 5 AU. The planetary configuration in late 2011 is represented in Figure 1.

[8] In September, the Sun emitted a series of powerful CMEs with large angular widths, directed toward Earth (Figure 2a). Three significant increases of the magnetic field and dynamic pressure, hereafter labelled A, B and C, were measured in the vicinity of Earth by the Wind spacecraft on 9, 17 and 26 September (Figure 2b, right), and each triggered intense auroral precipitation (Figure 2b, left). These events were predicted to reach Jupiter on 26 September, 2 and 10 October ±12 h respectively (Figure 2c, right). Associated Jovian radio auroral responses were identified by the STEREO spacecraft (orange-shaded intervals in Figure 2c, right), as illustrated on Figure 2c (left), close to the predicted times. Further comments on auroral observations at Earth and Jupiter are provided in the auxiliary material[1].

[9] HST observations of Uranus were scheduled approximately 1 month in advance in order to match the expected arrival of pressure fronts A, B and C in mid-November (Figure 2d, right). These were predicted with a ±1 day uncertainty, but interplanetary shocks merge into longer disturbances as they propagate with different speeds (Figure 2, right). This results, at 19 AU, in enhanced-pressure regions lasting 20–30 days, and separated by 20–30 days. As a result, 17 HST orbits (vertical blue lines in the bottom panel) were distributed over 3 weeks with a temporal resolution down to one third of a Uranus rotation (orbits 4, 5 and 6) and a coverage of all longitudes. HST alternately used STIS (solid blue lines) and ACS (dashed blue lines) instruments, that acquired a set of FUV images and spectra, from 115 to 175 nm, described in the auxiliary material. The last two images (Figure 2d, left), obtained around event C, reveal a bright spot on the planetary disc (orbit 17), not visible a day earlier (orbit 16).

3. Observations

[10] The auroral power radiated by Uranus is 2–3 times fainter than Saturn's, while the planet is located twice as far from the Sun. This results in a signal reduction of approximately an order of magnitude as observed from the Earth. We estimated a brightness in the HST FUV range derived from Voyager 2/UVS measurements of a few kR of H and H_2 auroral emission [*Herbert*, 2009], close to the HST sensitivity of ∼1 kR. This adds to ∼2 kR of dayside non-auroral emission (including dayglow and reflected sunlight), estimated from 1.4 kR of H Ly-α on average [*Clarke et al.*, 1986] and an assumed additional 30% contribution at long wavelengths.

[11] Clearest evidence of an auroral signal was obtained with STIS imaging using the clear (broadband) filter. Bright emissions (orbits 9 and 17) with intensities per pixel up to

---

[1]Auxiliary materials are available in the HTML. doi:10.1029/2012GL051312.
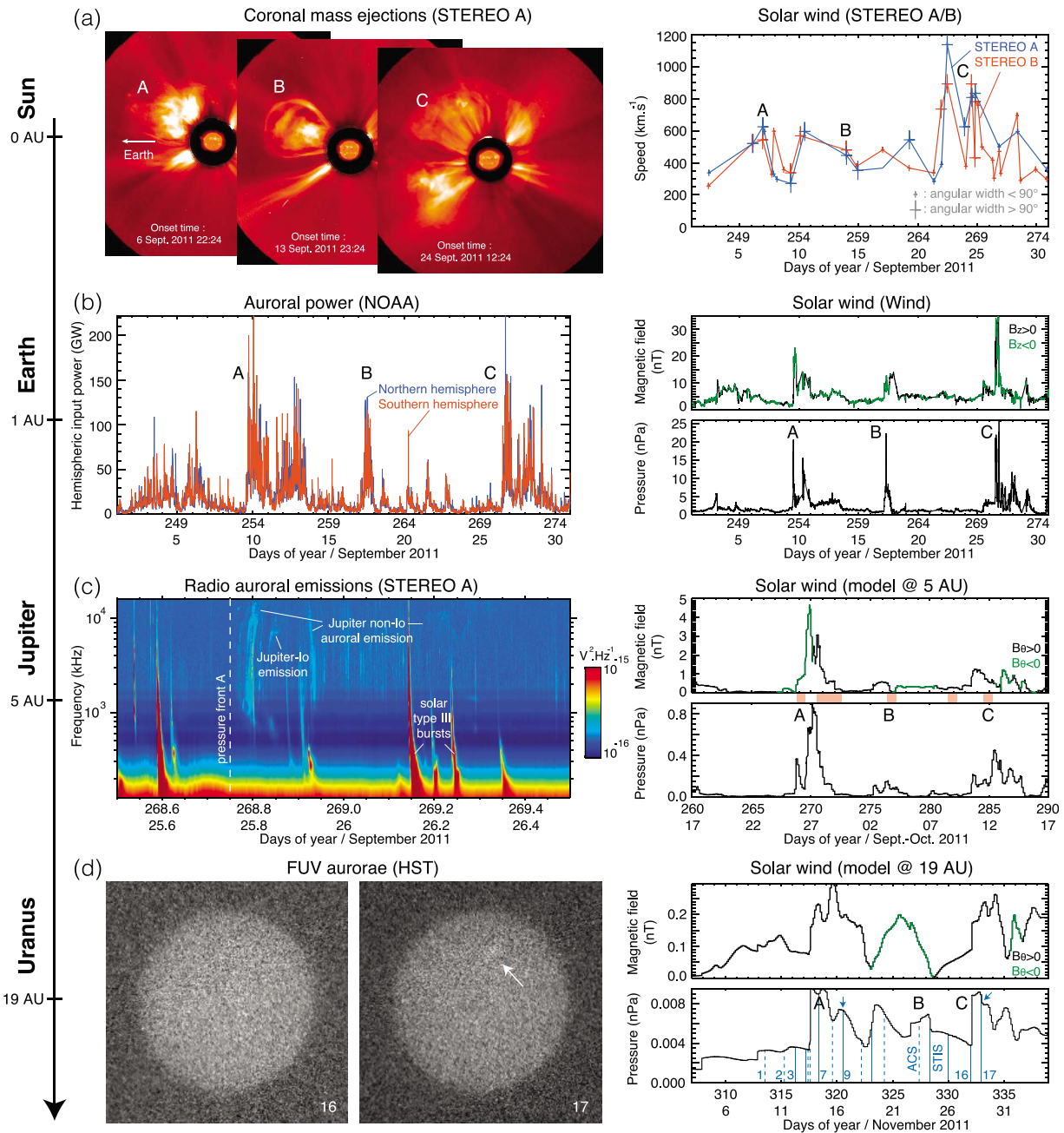
Figure 2. Multi-instruments observations of a series of (a) solar coronal mass ejections and their effects on auroral emissions of (b) Earth, (c) Jupiter and (d) Uranus in late 2011. Figure 2a displays CMEs emitted toward Earth in September 2011, as observed by STEREO/SECCHI cameras. (right) The median speed of Earth-directed CMEs measured with SECCHI-A and B (CACTus catalogue). Small (large) crosses refer to angular widths below (beyond) 90°. A, B and C mark powerful events of interest. (left) The CMEs emitted on 6, 13 and 24 September. Figures 2b (right), 2c (right), and 2d (right), show solar wind parameters as measured by Wind at 1 AU, and as propagated with the mSWiM code to 5 and 19 AU from the Sun. Each double panel displays (bottom) the dynamic pressure and (top) the magnetic field magnitude, in which green portions show negative values of B_z for the Earth (Geocentric Solar Ecliptic frame) or negative B_θ for Jupiter/Uranus (Sun-Planet spherical frame), favoring for the first two planets dayside reconnection and thus auroral activity. Figure 2b (left) shows the auroral precipitated powers in both terrestrial hemispheres in September, as obtained from polar measurements of NOAA satellites. Both hemispheric powers are well correlated with the solar wind dynamic pressure. Figure 2c (left) shows STEREO A/WAVES radio observations of Jupiter, corrected for light travel. Non-Io auroral emissions brighten from 16 MHz to 600 kHz a few hours before the predicted arrival of shock A. Jovian non-Io auroral emissions were recorded in response to all shocks within ±12 h (orange-shaded intervals in Figure 2c, right). Figure 2d (left) displays the last two HST images of Uranus of a campaign of 17 orbits, covering the arrival of pressure fronts A, B and C in November. Vertical solid (resp. dashed) blue lines in the right panel show the distribution of STIS (resp. ACS) snapshots, corrected for light travel. The arrows indicate the positive detections shown in Figures 3a and 3b. A bright spot is visible on image 17 (white arrow).
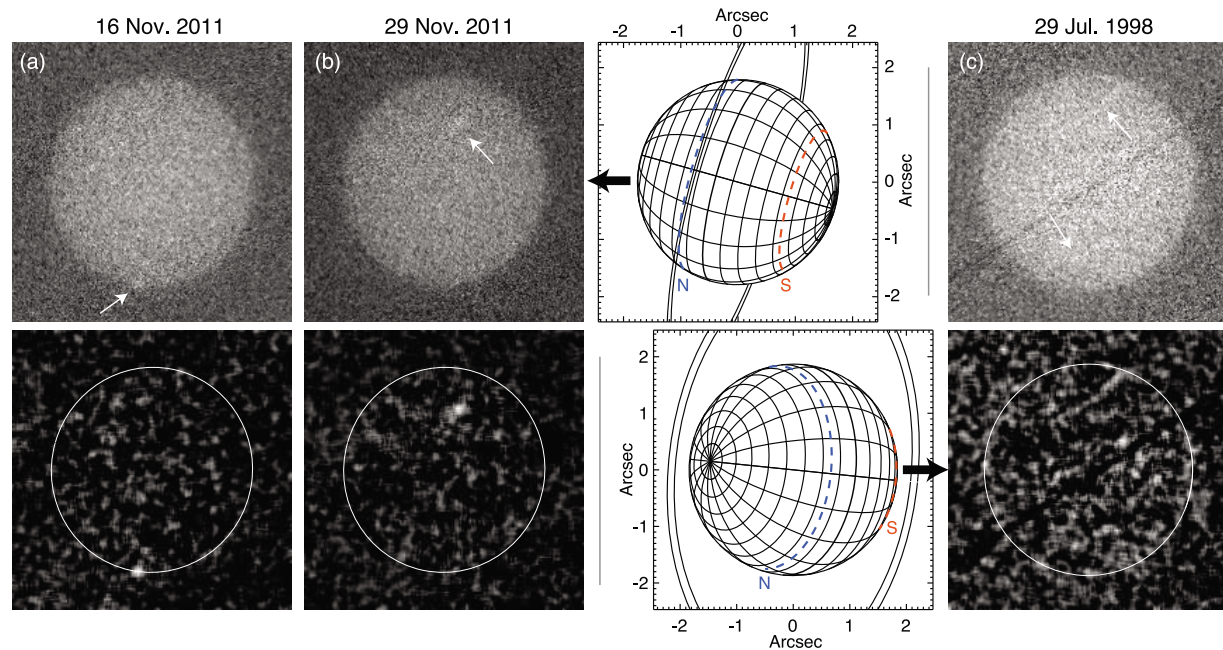
Figure 3. HST/STIS images acquired on (a) 16 Nov. 2011 15:32:10 UT, (b) 29 Nov. 2011 02:09:24 UT and (c) 29 Jul. 1998 06:07:43 UT, with the clear MAMA filter (spanning H_2 bands and H Ly-α) over 1000 s. (top) Raw images. (bottom) Same as Figure 3 (top) but after subtraction of a background of reflected sunlight and smoothing over 5 pixels (see auxiliary material). White arrows mark features of interest above the noise level: localized bright spots (Figures 3a and 3b), and northern/southern ring-like emissions (Figure 3c). Corresponding planetary configurations are shown with grids of planetocentric coordinates, where blue and red dashed lines indicating the latitude of the northern and southern magnetic poles.

3 to 5 standard deviations (σ) above the background level are visible in Figures 3a and 3b (see auxiliary material). Using the above disc brightness, the 3σ level yields ~1–2 kR. Despite ACS being more sensitive than STIS, it did not obtain comparable results. This could arise from either the timing of the ACS measurements and/or the STIS ability to be more solar-blind, offering better contrast. Interestingly, the bright spots in Figures 3a and 3b both lie at the same longitude (arbitrary) and latitude (between $-5°$ and $-15°$). This preferentially matches the visibility region of the N oval. Fainter signals of possible auroral origin were also observed around both magnetic poles and at longitudes consistent with the planetary rotation in two thirds of the STIS images. Orbits 17 and 9 lay 1 and 2.5 days after the pressure fronts C and A, respectively, but some northern fainter signal was already observed during orbit 7, 2 days prior to orbit 9. Using the STIS time-tag ability, we found that auroral signals in Figures 2a and 2b vary within the 1000 s duration of each image. The two hot spots mainly brighten during the first and second half of the two image intervals, respectively.

[12] We have also re-analyzed previous HST observations of Uranus. In July 1998, the planet was observed twice with STIS over 1.5 days. The image displayed in Figure 3c reveals two roughly continuous, distinct, rings of emission. While their intensity per pixel lies between 1 and 3σ above the noise level, the signal integrated along model ovals, fitted to their visible part with partial ellipses, reaches 4 to 5σ (see auxiliary material for details). N and S fitted emissions extend at latitudes from $-5°$ to $+70°$ and from $-15°$ to $+30°$, respectively, the N oval being larger than the S one, as expected. Both ovals are centered at around $+40°$ and $-11°$ latitude respectively, both similarly shifted by $+25°$ north of the latitude of their associated magnetic pole, and separated

by ~120° longitude, which is less than the expected 180° longitude difference. These results may be biased by the incomplete view of both ovals and/or their non-elliptical shape. No interplanetary shock was predicted close to observing dates. The time-tag mode revealed that the intensity of both ovals again varied over timescales of minutes. The N oval for instance intensified during the central 6 min of the ~17 min acquisition time. Signs of sporadic polar activity were also observed within both ovals.

4. Discussion

[13] Aurorae observed in 1986, 1998 and 2011 sample a quarter of a Uranus revolution around the Sun. Their characteristics provide insights on how diverse solar wind/magnetosphere configurations influence their mutual interaction and affect auroral processes.

[14] In 1986, the large tilt between the magnetic and rotation axis led the N and S magnetic poles rotating uniquely within the dayside and nightside hemispheres respectively, a unique situation in the solar system where the two dominant regimes governing magnetospheric plasma transport (solar wind convection and planetary rotation) act in perpendicular planes and are therefore decoupled. This gives rise to a significant helical magnetotail [*Behannon et al.*, 1987]. The prominence of nightside emissions, consistent with this configuration, led to consider auroral precipitation as driven by solar wind convection through nightside reconnection processes, as for the Earth [*Herbert*, 2009]. These emissions varied on few-day timescales [*Broadfoot et al.*, 1986], in agreement with typical convection-driven plasma residence times of 1–3 days [*Belcher et al.*, 1991]. Interestingly, we note that the

interval sampled by Voyager 2/UVS coincided with the passage of an interplanetary shock, which reached Uranus one day before closest approach and lasted for a week, and signs of substorm-like activity were identified in plasma measurements [*Sittler et al.*, 1987]. This compression may have triggered an Earth-type increase of auroral activity [e.g., *Boudouridis et al.*, 2005], in agreement with the outbound brightening of UV aurorae noticed by *Herbert and Sandel* [1994].

[15] The near-equinox conditions in 2011 yielded a very different situation, where N and S poles alternately nearly faced the sun (pole-on) and span a range of extreme magnetospheric configurations during each rotation. This novel, atypical, configuration of an asymmetric magnetosphere is investigated for the first time. We may expect increased variability in the geometry of open/closed field lines and shorter plasma residence times, which act against the formation of a stable magnetotail. Two clear auroral detections on 16 and 29 November, whose estimated brightness match the Voyager 2 results, occurred close to the predicted arrival of pressure fronts. But contrary to the Earth and Jupiter, whose auroral response roughly matched the shock duration, longer high-ram pressure conditions did not trigger similarly long auroral enhancement at Uranus. Instead, observed auroral spots were both well localized and highly variable, down to timescales of minutes. Such emissions could result from impulsive plasma injections through dayside reconnection with the interplanetary magnetic field, expected to be favored once per rotation. The investigation of the dynamic magnetic geometry, beyond the scope of this paper, is a key point to address.

[16] The magnetospheric situation in 1998 was intermediate between 1986 and 2011. Ring-like signatures visible on the dayside, under quiet solar wind conditions, illustrate yet another situation. Such emissions require precipitation of energetic particles over an extended range of longitudes. Their variability adds another strong constraint on the acceleration mechanism at work, possibly relying on a short-lived twisted magnetotail, which remains to be determined. This image also provides the first and single simultaneous view of both Uranian auroral ovals so far, obtained 12 years after their detection. It thus brings an opportunity to better constrain magnetic field models and to refine the determination of the rotation period [*Herbert*, 2009]. On the former topic, the centers of the model ovals differ somewhat from the expected position of the magnetic poles, though the determination of ovals' centers remains approximate. On the latter issue, the extension of the ULS system to make the N pole coinciding with the longitude of the N oval's center $\pm 45°$ yields a preliminary set of 8 putative rotation periods coincident with the interval : 17.24 ± 0.01 h, with an uncertainty improved to $\pm 4 \times 10^{-4}$ h (see auxiliary material). In both cases, more robust conclusions require the identification of at least one more oval, in available or future observations.

5. Conclusion

[17] Planetary auroral processes provide a useful remote diagnosis of solar wind activity throughout the heliosphere, even if the nature and the level of the auroral response vary with the characteristics of the magnetosphere. Here, we described the first unambiguous Earth-based detections of

Uranus' aurorae obtained with HST in 2011 and 1998. These are transient emissions of a few kR differing from other well-known planetary aurorae. Visible features are organized as dayside bright spots or roughly continuous ring-like emissions, that contrast with the tailward localized emissions measured by Voyager 2 in 1986. They indicate variations of the solar wind/magnetosphere interaction at very different timescales, which we assign to changes of the magnetospheric configuration, although the auroral acceleration mechanism(s) operating during these observations remain to be identified.

[18] These results open a wide field of investigations on this unique and poorly understood magnetosphere. In parallel, the analysis of NIR observations obtained simultaneously with HST on 24 and 25 November using the ground-based IRTF telescope, as part of long-term monitoring of Uranian H_3^+ emission [*Melin et al.*, 2011], will enable the identification of any IR auroral contribution (H. Melin et al., manuscript in preparation, 2012).

[19] More than a quarter of century after the Voyager 2 flyby, the interest of a large community in ice giants in general, and the Uranus system in particular, has recently been renewed through a mission concept submitted to ESA in 2011 [*Arridge et al.*, 2012]. But in the absence of any exploring probe yet planned, and without considering the travel time needed to reach the planet (12–15 years cruise), Earth-based UV observations remain a unique tool to remotely probe Uranus' unique aurorae and magnetosphere.

[21] The Editor thanks two anonymous reviewers for assisting in the evaluation of this paper.

References

Arridge, C. S., et al. (2012), Uranus Pathfinder: Exploring the origins and evolution of Ice Giant planets, *Exp. Astron.*, doi:10.1007/s10686-011-9251-4, in press.

Behannon, K. W., R. P. Lepping, E. C. Sittler Jr., N. F. Ness, B. H. Mauk, S. M. Krimigis, and R. L. McNutt Jr. (1987), The magnetotail of Uranus, *J. Geophys. Res.*, 92, 15,354–15,366, doi:10.1029/JA092iA13p15354.

Belcher, J. W., et al. (1991), The plasma environment of Uranus, in *Uranus*, pp. 780–830, Univ. of Ariz. Press, Tucson.

Boudouridis, A., E. Zesta, L. R. Lyons, P. C. Anderson, and D. Lummerzheim (2005), Enhanced solar wind geoeffectiveness after a sudden increase in dynamic pressure during southward IMF orientation, *J. Geophys. Res.*, 110, A05214, doi:10.1029/2004JA010704.

Broadfoot, A. L., et al. (1986), Ultraviolet spectrometer observations of Uranus, *Science*, 233, 74–79, doi:10.1126/science.233.4759.74.

Clarke, J. T., et al. (1986), Continued observations of the H Ly α emission from Uranus, *J. Geophys. Res.*, 91, 8771–8781, doi:10.1029/JA091iA08p08771.

Clarke, J. T., et al. (2009), Response of Jupiter's and Saturn's auroral activity to the solar wind, *J. Geophys. Res.*, 114, A05210, doi:10.1029/2008JA013694.

Connerney, J. E. P., M. H. Acuña, and N. F. Ness (1987), The magnetic field of Uranus, *J. Geophys. Res.*, 92, 15,329–15,336, doi:10.1029/JA092iA13p15329.

Desch, M. D., et al. (1986), The rotation period of Uranus, *Nature, 322,* 42–43, doi:10.1038/322042a0.

Herbert, F. (2009), Aurora and magnetic field of Uranus, *J. Geophys. Res., 114,* A11206, doi:10.1029/2009JA014394.

Herbert, F., and B. R. Sandel (1994), The Uranian aurora and its relationship to the magnetosphere, *J. Geophys. Res., 99,* 4143–4160, doi:10.1029/93JA02673.

Lam, H. A., et al. (1997), Variation in the H_3^+ emission of Uranus, *Astrophys. J. Lett., 474,* L73, doi:10.1086/310424.

Melin, H., et al. (2011), Seasonal variability in the ionosphere of Uranus, *Astrophys. J., 729,* 134, doi:10.1088/0004-637X/729/2/134.

Ness, N. F., et al. (1986), Magnetic fields at Uranus, *Science, 233,* 85–89, doi:10.1126/science.233.4759.85.

Prangé, R., et al. (2004), An interplanetary shock traced by planetary auroral storms from the Sun to Saturn, *Nature, 432,* 78–81, doi:10.1038/nature02986.

Sittler, E. C., Jr., K. W. Ogilvie, and R. Selesnick (1987), Survey of electrons in the Uranian magnetosphere: Voyager 2 observations, *J. Geophys. Res., 92,* 15,263–15,281, doi:10.1029/JA092iA13p15263.

Trafton, L. M., et al. (1999), H_2 Quadrupole and H_3^+ emission from Uranus: The Uranian thermosphere, ionosphere, and aurora, *Astrophys. J., 524,* 1059–1083, doi:10.1086/307838.

Zieger, B., and K. C. Hansen (2008), Statistical validation of a solar wind propagation model from 1 to 10 AU, *J. Geophys. Res., 113,* A08107, doi:10.1029/2008JA013046.

J. Aboudarham, B. Cecconi, L. Lamy, R. Prangé, and P. Zarka, LESIA, Observatoire de Paris, CNRS, UPMC, Université Paris Diderot, 5, Place Jules Janssen, F-92190 Meudon CEDEX, France. (laurent.lamy@obspm.fr)

N. Achilleos and P. Guio, Department of Physics and Astronomy, University College London, Gower Street, London WC1E 6BT, UK.

N. André, Institut de Recherche en Astrophysique, 9, avenue du Colonel Roche, F-31028 Toulouse CEDEX, France.

G. Ballester, Lunar and Planetary Laboratory, University of Arizona, 1629 E. University Blvd., Tucson, AZ 85721, USA.

M. Barthélémy, Institut de Planétologie et d'Astrophysique de Grenoble, BP 53, F-38041 Grenoble CEDEX 9, France.

G. Branduardi-Raymont, Mullard Space Science Laboratory, University College London, Dorking RH5 6NT, UK.

J. T. Clarke, Center for Space Physics, Boston University, 725 Commonwealth Ave., Boston, MA 02215, USA.

S. W. H. Cowley, H. Melin, J. D. Nichols, and T. S. Stallard, Department of Physics and Astronomy, University of Leicester, University Road, Leicester LE1 7RH, UK.

M. K. Dougherty, Blackett Laboratory, Imperial College London, Exhibition Road, London SW7 2BZ, UK.

R. Gladstone, Southwest Research Institute, 6220 Culebra Rd., PO Drawer 28510, San Antonio, TX 78238, USA.

K. C. Hansen, Department of Atmospheric, Oceanic and Space Sciences, University of Michigan, 2455 Hayward St., Ann Arbor, MI 48109, USA.